



Solution-Processed Transparent Superhydrophobic Protection Layers for Enhancing the Device Reliability of Flexible Organic Optoelectronics

Daekyoung Yoo, Keehoon Kang, Youngrok Kim, Heebeom Ahn, Woocheol Lee, Jinsu Pak, Seungjun Chung,* and Takhee Lee*

Organic materials and devices have attracted great attention for implementation of flexible and transparent electronics applications. However, further easy-to-manage organic devices with acceptable environmental reliability in open air are desirable. Specifically, because water-based threats and particle contamination can degrade the functions of organic optoelectronics, introducing a superhydrophobic protection layer onto organic devices, which can eliminate issues via excellent water repellency, is necessary. In this study, surface-engineered TiO₂ nanoparticles dispersed in a highly fluorinated solvent are deposited on organic devices using organo-compatible solution processing. The optimization of the TiO₂ nanoparticle layer, such as the surface roughness and thickness of the film, enables the realization of a transparent superhydrophobic layer; therefore, the film can be utilized in transparent organic optoelectronics, especially in phototransistor applications. The transparent superhydrophobic layer exhibits good water repellency without critical delamination issues even during mechanical deformation, such as bending and stretching tests. Flexible organic phototransistors with the transparent superhydrophobic layer show a self-cleaning ability against harmful contaminants on the topmost surface, achieved by dropping water droplets. This work can provide a feasible solution to maintaining transparent and flexible organic devices with improved environmental reliability.

improved environmental stability indicates that organic electronics could be utilized in the open air beyond controlled laboratory conditions.^[8–11] To achieve better reliability from the perspective of devices, one of the key challenges is to integrate protection layers effective against external threats encountered in daily conditions. In this regard, introducing superhydrophobic layers showing a water contact angle above 150° onto organic electronics is an attractive solution because excellent water repellency can efficiently remove particle contamination or water-based threats via a self-cleaning ability.^[8,12–15] Recently, we reported that superhydrophobic protection layers can improve the environmental stability of organic field-effect transistors (FETs).^[8] However, the reported opaqueness of the layer with a thickness above 10 μm can be a critical obstacle to utilization in thin-film optoelectronic device applications. To provide transparency to the protection layers while preserving the organo-compatibility, optimization of the thickness and surface roughness of the superhydrophobic layers

1. Introduction

In recent decades, organic electronic materials have paved a promising route for realizing large-area flexible device applications with low-cost solution processing.^[1–7] Specifically, their

is required to obtain enhanced transmittance via reduced light scattering.^[14–16] In addition, preserving the superhydrophobicity under various types of mechanical deformation, thermal stress, and light exposure is necessary for integration to realize practical flexible applications.

Here, we report solution-processed transparent superhydrophobic protection layers for enhancing the reliability of organic optoelectronic devices. Functionalized titanium dioxide (TiO₂) nanoparticles with fluorinated alkyl silane were dispersed in a highly fluorinated solvent; therefore, they could be directly deposited on organic phototransistors without any additional pretreatment. By controlling the surface roughness of the TiO₂ nanoparticle layer, the prepared layer exhibited a high transmittance of ~80% in the visible wavelength range (>400 nm) while maintaining the superhydrophobicity that provided an excellent self-cleaning ability. In addition, various liquids with lower surface tension than water could also roll off of the surface, demonstrating excellent liquid repellency. The superhydrophobicity was well maintained under temperature-acceleration tests until

D. Yoo, Dr. K. Kang, Y. Kim, H. Ahn, W. Lee, J. Pak, Prof. T. Lee
Department of Physics and Astronomy
Institute of Applied Physics
Seoul National University
Seoul 08826, Korea
E-mail: tlee@snu.ac.kr

Dr. S. Chung
Photo-Electronic Hybrids Research Center
Korea Institute of Science and Technology
Seoul 02792, Korea
E-mail: seungjun@kist.re.kr

 The ORCID identification number(s) for the author(s) of this article can be found under <https://doi.org/10.1002/admt.202000449>.

DOI: 10.1002/admt.202000449

the decomposition temperature of the fluorinated alkyl silane molecules attached to the TiO₂ nanoparticles was reached and under exposure to a high-intensity laser light for 3 d. Although there have been previous results of nanoparticle-based superhydrophobic layers with engineering the surface roughness and particle sizes,^[17,18] we report further deep studies on superhydrophobicity based on surface structures which allow outstanding repellency against small water drops having a volume of a few μL. The transparent superhydrophobic layers were implemented on 6,13-bis(triisopropylsilylethynyl) pentacene (TIPS-pentacene) organic phototransistors. TIPS-pentacene phototransistors with the transparent self-cleaning layer exhibited enhanced environmental reliability against water droplets and particle contamination.

2. Results and Discussion

To integrate transparent superhydrophobic layers onto organic optoelectronic devices, we prepared a solution by mixing 1 g of 1*H*,1*H*,2*H*,2*H*-perfluorooctyltriethoxysilane (PFOTES) and 1 g of TiO₂ nanoparticles (particle size of ≈20 nm) into a highly fluorinated solvent, 3-ethoxy-1,1,1,2,3,4,4,5,5,6,6,6-dodecafluoro-2-trifluoromethylhexane (HFE-7500). PFOTES was attached to TiO₂ nanoparticles in the fluorinated solution through the chemical reaction between the silanol groups of PFOTES and the hydroxyl groups on the surface of the TiO₂ nanoparticles.^[8,13,19,20] The prepared solution including PFOTES-attached TiO₂ nanoparticles was directly spin-coated onto TIPS-pentacene phototransistors in ambient conditions at a rotation speed of 500 rpm for 30 s (Figure 1a). The PFOTES containing the trifluoromethyl (–CF₃)

group (Figure 1b) with an extremely low surface tension of 6.7 mJ m^{–2} and the deposited TiO₂ nanoparticle layer with a low surface roughness (root-mean-square (RMS) roughness of ≈30 nm in a 1 × 1 μm² area, shown in Figure S1, Supporting Information) can simultaneously offer both superhydrophobicity and transparency.^[14–18,20–22] Because the spin-coated TiO₂ nanoparticle layer was not sufficiently transparent in the visible spectrum, a rinsing process was conducted with a highly fluorinated solvent based on HFE-7200 (mixture of the isomers 1-ethoxy-1,1,2,2,3,3,4,4,4-nonaffluorobutane and 1-ethoxy-1,1,2,3,3,3-hexafluoro-2-(trifluoromethyl) propane) and acetone in a volume ratio of 10:1 to remove excess TiO₂ nanoparticles, resulting in a transparent superhydrophobic layer. Typically, because the fluorinated solvent does not physically or chemically damage organic materials, the superhydrophobic layer could be deposited on TIPS-pentacene organic phototransistors without interfering with the underlying organic layers (Figure 1a),^[8,23] which could not be achieved in previously reported works using nonpolar or ethanol-based solvents.^[17,18]

While a water contact angle of 89° was observed on the pristine TIPS-pentacene semiconductor film (Figure 1c), the PFOTES-attached TiO₂ nanoparticle layer on the organic semiconducting film showed a high water contact angle up to 166° without transmittance degradation (Figure 1d). Our transparent superhydrophobic layers could be uniformly deposited on a variety of flexible substrates, for example, polyethylene terephthalate (PET), poly(dimethylsiloxane) (PDMS), and commercially available paper substrates, exhibiting high water contact angles >150°, which are comparable to the results of previously reported superhydrophobic layers (Figures S2–S5, Supporting Information).^[8,12–18,20,21,24–27]

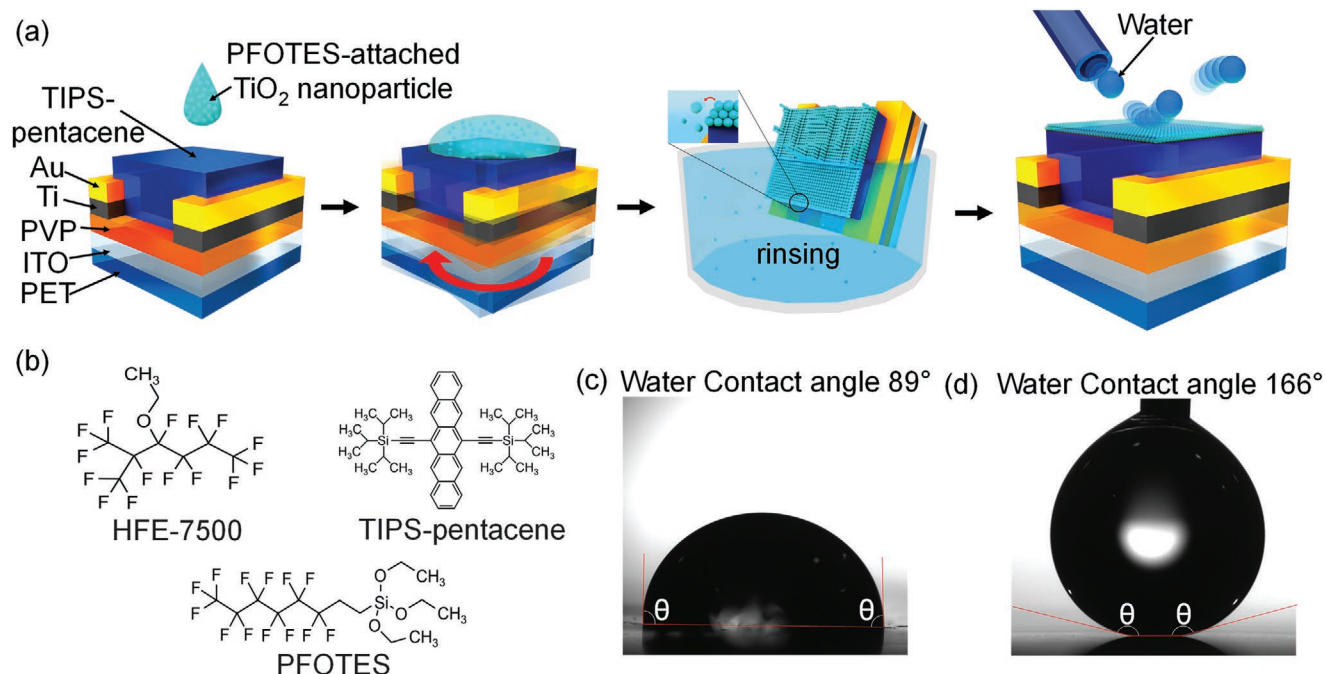


Figure 1. Transparent superhydrophobic layers for organic phototransistors. a) Schematic images of the deposition of the transparent superhydrophobic layer onto an organic phototransistor. b) Molecular structures of HFE-7500, TIPS-pentacene, and PFOTES. c) Optical image of the water contact angle on a TIPS-pentacene semiconducting layer. f) Optical image of the water contact angle on the transparent superhydrophobic layer on the TIPS-pentacene layer.

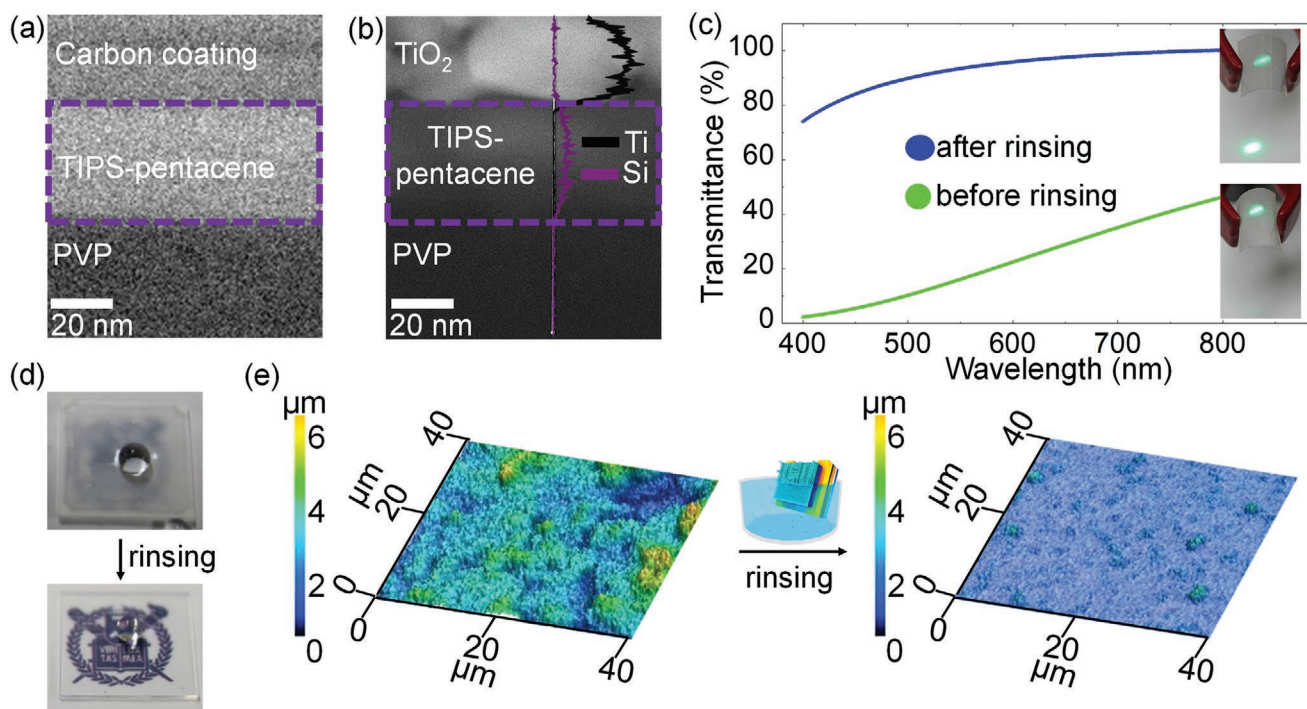


Figure 2. Transmittance and surface profile of the organo-compatible superhydrophobic transparent layer. a,b) TEM images of TIPS-pentacene layers w/o and w/the PFOTES-attached nanoparticle layer. c) Transmittance of the transparent and opaque superhydrophobic layers under visible light; the inset figures are optical images for the transmittance of 520 nm laser light. d) Optical images of water droplets on the opaque superhydrophobic layer (top) and transparent superhydrophobic layer (bottom). e) 3D laser profiler images of the PFOTES-attached TiO_2 nanoparticle layer before rinsing (left) and after rinsing (right).

From the transmission electron microscopy (TEM) images shown in **Figure 2a,b**, we did not observe any physical or chemical damage to the TIPS-pentacene layer after depositing the TiO_2 nanoparticle layer. The PFOTES-attached TiO_2 nanoparticle layer showed high transparency with a transmittance of $\approx 80\%$ for wavelengths over 400 nm after the rinsing process, which is comparable to the visible light transmittances of previously reported transparent superhydrophobic layers,^[14–18,20,24,25,27] whereas unrinsed (opaque) films showed much lower transmittances (**Figure 2c**).

The inset figures in **Figure 2c** indicate that most of the light with a wavelength of 520 nm (green) from a laser could not pass through the opaque superhydrophobic layer due to light scattering, whereas the visible light passed through the transparent superhydrophobic layer (see also **Figure S6**, Supporting Information). The superhydrophobicity was well maintained for the transparent layer even after rinsing off the unbound TiO_2 nanoparticles, based on the spherical water droplet clearly observed on the layer (**Figure 2d**). Detailed analysis of the changes in the surface roughness before and after the rinsing process was conducted by using 3D laser profilometry, scanning electron microscopy (SEM), and atomic force microscopy (AFM) (**Figure 2e** and **Figures S5** and **S7–S9**, Supporting Information). The surface of the TiO_2 nanoparticle layer characterized by the 3D laser profiler showed obvious differences in the surface roughness and particle aggregation for the opaque and transparent superhydrophobic layers (**Figure 2e**). The film thicknesses of the opaque and transparent superhydrophobic

layers were ≈ 4.27 and $0.28 \mu\text{m}$, respectively (see also **Figure S8**, Supporting Information). Consequently, the RMS roughness of the transparent superhydrophobic layer was drastically reduced to ≈ 30 nm in a scan area of $1 \times 1 \mu\text{m}^2$, whereas that of the opaque superhydrophobic layer was ≈ 110 nm for the same scan size (**Figures S1**, **S5**, and **S9**, Supporting Information). A sub-100 nm RMS roughness leads to high transparency by significantly reducing the light scattering arising from the surface roughness (**Table S1**, Supporting Information).^[16–18,20,24–27] In this context, Mie scattering of visible light could be suppressed in our TiO_2 nanoparticle layer compared to the previous result, leading to its high transmittance in the visible spectrum because the surface roughness and nanoparticle sizes were much smaller than the visible light wavelengths.^[14,16,28]

The controlled surface roughness enabled us to achieve water repellency even for small water droplets having a volume of less than $1 \mu\text{L}$ (**Figure 3a,b** and **Figure S10**, Supporting Information). The Laplace pressure increases as the size of a water droplet decreases; thus, small-sized water droplets can permit easy filling of air gaps among the surface roughness peaks of superhydrophobic layers.^[12,29] In other words, although water droplets with a small diameter can show high contact angles on a superhydrophobic surface, they cannot be easily rolled off from the surfaces.^[12,29] To provide water repellency against sub- μL -volume droplets, the distance between the surface roughness peaks should be minimized.^[12,29] From the surface roughness measured by AFM, the average peak-to-peak distance of the nanoparticles was found to be less than $5 \mu\text{m}$,

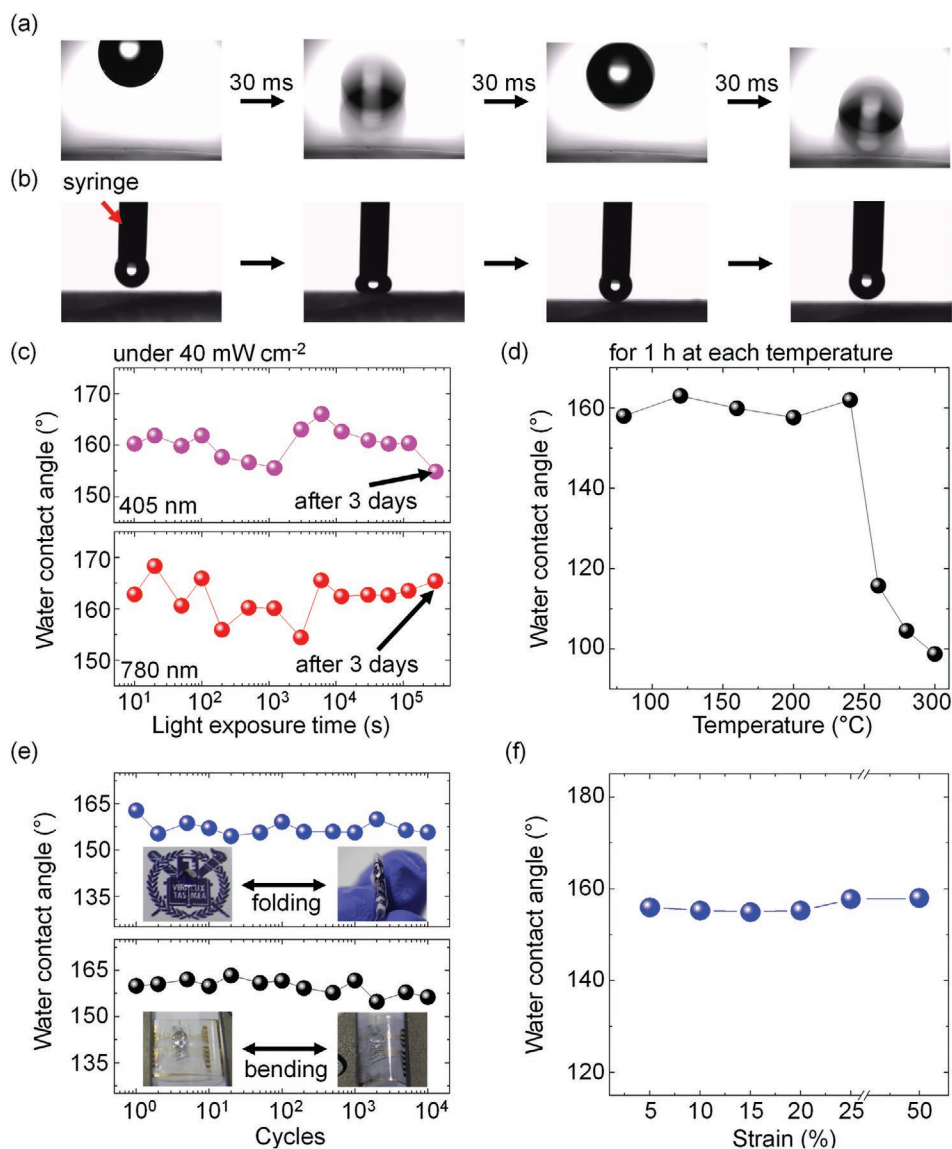


Figure 3. Water repellency and mechanical durability of the transparent superhydrophobic layer. a) Optical images of a water droplet bouncing on the superhydrophobic surface. b) Small water droplets from a syringe did not pin to the superhydrophobic surface. c) Water contact angles of the transparent superhydrophobic layers under light stress induced by visible light lasers with 405 and 720 nm wavelengths for 3 d. d) Water contact angles of the transparent superhydrophobic layers under thermal stress induced by increasing the temperature from 80 to 300 °C for 1 h. e) Water contact angles of the transparent superhydrophobic layers after folding and bending cycles. f) Water contact angles of the transparent superhydrophobic layer under stretched conditions up to 50% strain.

and the average peak-to-valley height was found to be $\approx 0.1 \mu\text{m}$ (Figure S11, Supporting Information). Assuming that the rough surface is a pillar array, the critical radius of water droplet curvature below which a water droplet cannot be rolled off was estimated to be $\approx 100 \mu\text{m}$ (corresponding to a volume of $\approx 4 \times 10^{-3} \mu\text{L}$) from the following equation^[29]

$$1/R_{\text{cr}} = 4h_0 / (w_0^4 + 4h_0^4)^{0.5} \quad (1)$$

where R_{cr} , w_0 , and h_0 denote the critical radius of the water droplet curvature between pillars, the peak-to-peak distance, and the peak-to-valley height, respectively. This result indicates that the surface roughness of our transparent protection layer

was sufficient to provide repellency of water droplets having a volume less than $1 \mu\text{L}$.^[12,29] Furthermore, our superhydrophobic layer also showed repellency against liquids with lower surface tension than water due to its structural properties (Figures S12–S14, Supporting Information).^[30]

The superhydrophobicity of our transparent protection layer was well maintained under light, thermal and mechanical stress. When superhydrophobic layers were exposed to 405, 520, 658, and 780 nm laser light with an intensity of 40 mW cm^{-2} , which is sufficient for evaluating organic optoelectronics,^[3] for 3 d, the contact angles were still above 150° regardless of the laser wavelength (Figure 3c and Figures S15 and S16, Supporting Information). Additionally, the transparent

superhydrophobic layers showed thermal resistance up to 240 °C for 1 h and degraded at temperatures above 250 °C (Figure 3d). This transition temperature was close to the desorption temperature of PFOTES attached to the TiO₂ nanoparticles for providing low surface tension.^[8,22,31] We also evaluated the mechanical stability of the transparent superhydrophobic layer. During mechanical folding and bending with a curvature radius up to 3 mm of transparent superhydrophobic layers on paper and PET substrates, respectively, the layers maintained high water contact angles over the 10⁴ times cycling test, even under stretched conditions up to 50% on a PDMS substrate, because the peak-to-peak distance and peak-to-valley height were sufficient for realizing superhydrophobicity during the mechanical deformation (Figure 3e,f and Figures S17–S19, Supporting Information). This outstanding mechanical durability was attributed to the well-preserved surface without critical delamination issues (Figures S20 and S21, Supporting Information). These results indicate that our strategy for achieving a self-cleaning ability can be utilized for arbitrarily shaped objects or stretchable electronics.

With these beneficial advantages, we deposited the transparent superhydrophobic layer onto TIPS-pentacene

phototransistors to enhance the reliability against water-based threats and provide a self-cleaning ability. Due to the use of fluorinated solvents and room temperature processing, the transparent superhydrophobic layers can be directly employed in organic devices without any damage or dewetting issues.^[8,23]

Figure 4 shows the transfer curves (drain–source current vs gate voltage, I_{DS} – V_{GS}) of TIPS-pentacene thin-film transistors (TFTs) obtained for V_{GS} ranging from 60 to –60 V at a fixed drain–source voltage (V_{DS}) of –60 V. Under laser light exposure, the threshold voltage and on-state current changed depending on the wavelength and intensity of the laser light. Under light illumination with different wavelengths of 450, 520, and 635 nm, which represent blue, green, and red light, respectively, and a light intensity of 1500 $\mu\text{W cm}^{-2}$, the transfer curves shifted toward positive gate voltage for both the TIPS-pentacene phototransistors w/and w/o the transparent superhydrophobic layer, as shown in Figure 4a,d. When exposed to laser light with a shorter wavelength, a more positive shift of the transfer curve was achieved for both the organic phototransistors w/and w/o the transparent superhydrophobic layer. A threshold voltage shift was also observed with changing light intensity when the wavelength was fixed at 450 nm (Figure 4b,e). These behaviors

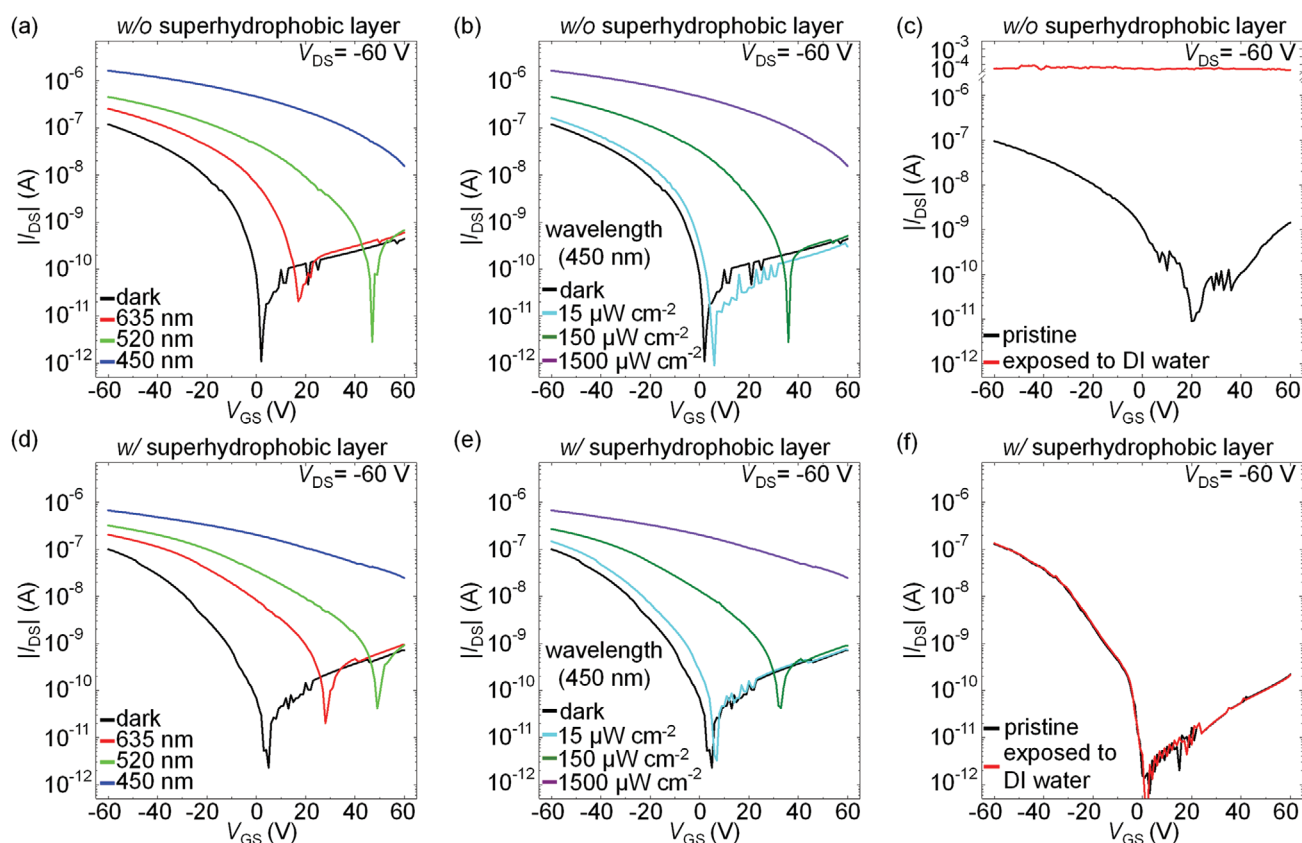


Figure 4. Representative transfer curves of TIPS-pentacene organic phototransistors w/and w/o the transparent superhydrophobic layer under light illumination. a,d) Transfer curves on the semilogarithmic scale for TIPS-pentacene organic phototransistors w/and w/o the transparent superhydrophobic layer under dark conditions and light illumination with different wavelengths at a fixed light intensity of 1500 $\mu\text{W cm}^{-2}$ in ambient conditions. b,e) Transfer curves on the semilogarithmic scale for TIPS-pentacene organic phototransistors w/and w/o the transparent superhydrophobic layer under dark conditions and light illumination with various light intensities from 15 to 1500 $\mu\text{W cm}^{-2}$ at a fixed wavelength of 450 nm in ambient conditions. c,f) Transfer curves on the semilogarithmic scale for TIPS-pentacene phototransistor w/and w/o the transparent superhydrophobic layer before and after exposure to DI water in ambient conditions.

are induced by the increase in the carrier density due to more electron–hole pairs being photogenerated by light illumination with a shorter wavelength or a greater intensity. More data about the shift in the threshold voltage of the TIPS-pentacene phototransistors are provided in Figure S22 (Supporting Information). Without degradation of the film transparency, our superhydrophobic layer could protect the electrical characteristics of organic semiconductor devices against water-based threats. Ionic conduction can cause extra current paths in the semiconducting channel region. As shown in Figure 4c, the unprotected TIPS-pentacene phototransistor exhibited an I_{DS} of 10^{-4} A without a gating capacity when exposed to water. However, the protected counterparts showed consistent electrical characteristics, including on/off ratio and field-effect mobility, before and after exposure to water because the protection layer effectively repelled water droplets (Figure 4f). This behavior was also beneficial for achieving a self-cleaning ability of organic electronic devices. Because water droplets could not adhere to the surface of the protection layers, excellent water repellency was feasible, enabling the elimination of undesirable opaque hindrances such as harmful particle contamination. Figure 5a clearly shows that heavy soil that blocked out the incident light was efficiently removed from the surface of protected TIPS-pentacene phototransistors by only dropping water droplets. Therefore, photoresponsive performances of TIPS-pentacene phototransistors consistent with those of their counterparts

without heavy soil on the surface could be achieved after self-cleaning, as shown in Figure 5b,c. These abilities can lead to further easy management of organic devices working in open air.

3. Conclusion

In summary, we report an enhanced environmental reliability of organic optoelectronic devices against water-based threats, obtained by introducing solution-processed transparent TiO_2 nanoparticle-based superhydrophobic layers. This protection layer could be directly deposited onto organic materials by using facile solution processing. The rinsing process allowed control of the surface roughness of the superhydrophobic layers, which is a key approach to realizing transparent layers by minimizing light scattering. In addition, the superhydrophobicity was well preserved under accelerated light, thermal and mechanical stress. With these favorable properties of the transparent superhydrophobic layers, further reliable TIPS-pentacene phototransistors were demonstrated to maintain their optoelectronic properties under water-based threats. In addition, the excellent water repellency could provide a self-cleaning ability involving only dropping water droplets to efficiently eliminate undesirable particle contamination. This work can pave the way to realizing more practical organic optoelectronics with transparent superhydrophobic protection layers in open air.

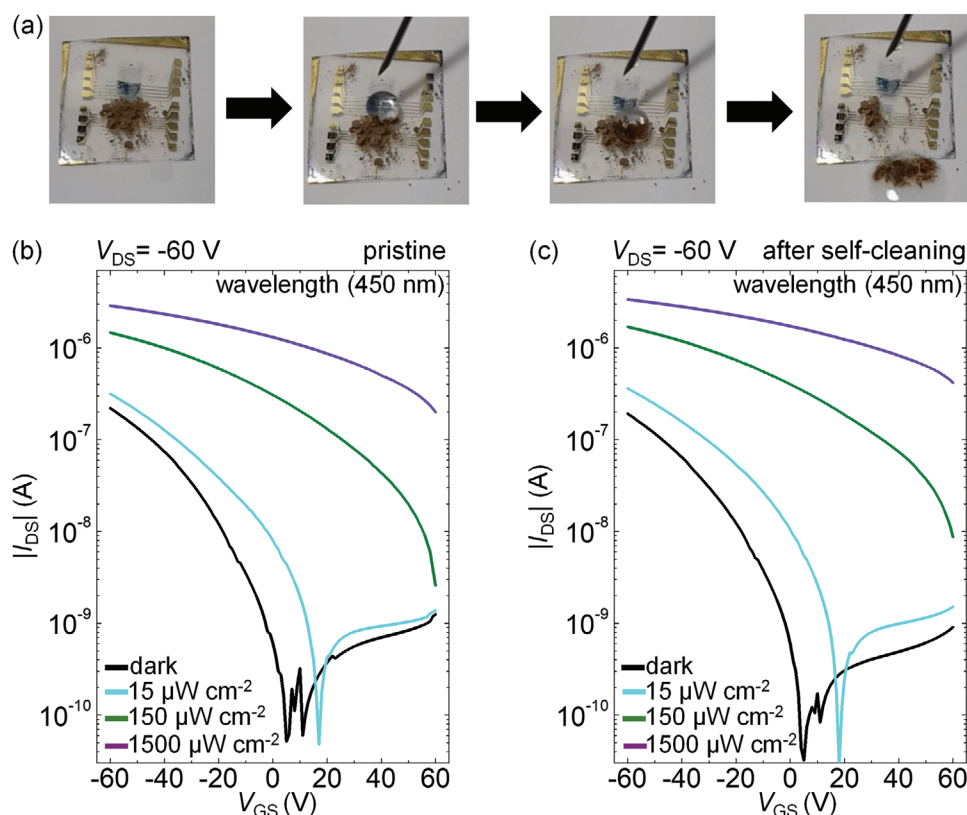


Figure 5. Self-cleaning ability of a TIPS-pentacene phototransistor due to the introduction of the transparent superhydrophobic layer. a) Elimination of soil on a TIPS-pentacene phototransistor with the transparent superhydrophobic layer by dropping water droplets. b,c) Transfer curves on the semi-logarithmic scale for TIPS-pentacene organic phototransistors with the transparent superhydrophobic layer before and after the self-cleaning process under dark conditions and light illumination with various light intensities from 15 to $1500 \mu\text{W cm}^{-2}$ at a fixed wavelength of 450 nm.

4. Experimental Section

Preparation of Transparent Superhydrophobic Protection Layers: To prepare the transparent superhydrophobic protection layer, HFE-7500 was purchased from 3M and titanium (IV) oxide with a primary particle size of 21 nm and PFOTES from Sigma-Aldrich. First, 1.0 g of PFOTES was placed into 15 mL of HFE-7500, and then, it was mixed with 1.0 g of TiO₂ nanoparticles. After exposing the solution to an ultraviolet lamp for 1 h for better dispersion, the solution was spin-coated onto organic optoelectronic devices at a spin speed of 500 rpm for 30 s. Finally, the devices were dipped into a rinsing solution composed of HFE-7200 (100 mL) and acetone (10 mL) for 5 s.

Fabrication of Organic Phototransistors: For fabricating TIPS-pentacene phototransistors, indium tin oxide (ITO)-coated PET substrates (purchased from Sigma-Aldrich) were sequentially cleaned with acetone, isopropanol, and deionized water for 10 min in each solution. The cleaned ITO-coated PET substrates were exposed to an ultraviolet ozone cleaner for 5 min, which enhanced the film uniformity. A solution containing 20 wt% poly(4-vinylphenol) (PVP, Mw = 25 000 g mol⁻¹, Sigma-Aldrich) and 5 wt% (PMF, number-average molecular weight (Mn) ≈ 432 g mol⁻¹, Sigma-Aldrich) dissolved in propylene glycol methyl ether acetate (PGMEA) was spin-coated onto the cleaned ITO at a 500 rpm rate for 5 s and 2000 rpm for 40 s to form the gate dielectric. Then, it was sequentially annealed at 100 °C for 10 min and 210 °C for 10 min. Ti (5 nm)/Au (60 nm) source/drain electrodes with channel widths and lengths of 300 μm and 50 μm, respectively, were deposited onto the PVP gate dielectric layers using an electron-beam evaporator at a rate of 0.5 Å s⁻¹. Then, 0.5 wt% TIPS-pentacene dissolved in toluene was drop-cast onto the patterned Ti/Au source/drain electrodes and then dried in air for 1 h.

Environmental Reliability Tests: To investigate the stability of the transparent superhydrophobic layers under light stress, they were exposed to visible laser light with a power of 40 mW cm⁻² and a spot size of 0.2 cm² (wavelengths of 405, 520, 658, and 780 nm). The thermal reliability was examined by measuring the water contact angles on the transparent superhydrophobic layers after annealing on a hot plate with increasing temperature from 80 to 300 °C for 1 h. Mechanical stability tests of 10⁴ repetitive bending cycles at bending radii of 3, 5, and 10 mm were conducted to investigate the mechanical reliability using a bending machine (Hansung Systems, Inc.).

Characterization: Electrical measurements were conducted using a semiconductor analyzer system (Model 4200-SCS, Keithley Inc.) at room temperature in a probe station (JANIS Model ST-500) under ambient conditions. Lasers of 558 and 665 nm wavelengths were used to evaluate the organic phototransistor devices. The optical transmittance of the transparent superhydrophobic layers was measured using a spectrophotometer (MAPADA UV-3100PC). AFM (Nanonavi E-Sweep) was used to analyze the surface roughness.

Supporting Information

Supporting Information is available from the Wiley Online Library or from the author.

Acknowledgements

The authors appreciate the financial support of the National Creative Research Laboratory program (Grant No. 2012026372) through the Korean National Research Foundations (NRF) funded by the Korean Ministry of Science and ICT. S.C. appreciates the support by the Korea Institute of Science and Technology (KIST) Future Resource Research Program (2E30160).

Conflict of Interest

The authors declare no conflict of interest.

Keywords

superhydrophobic layers, organic semiconductors, nanoparticles, reliability, organic optoelectronic devices

Received: May 10, 2020
Published online: June 24, 2020

- [1] S. R. Forrest, *Nature* **2004**, *428*, 911.
- [2] T. Sekitani, T. Yokota, U. Zschieschang, H. Klauk, S. Bauer, K. Takeuchi, M. Takamiya, T. Sakurai, T. Someya, *Science* **2009**, *326*, 1516.
- [3] K.-J. Baeg, M. Binda, D. Natali, M. Caironi, Y.-Y. Noh, *Adv. Mater.* **2013**, *25*, 4267.
- [4] B. Lucas, T. Trigaud, C. Videlot-Ackermann, *Polym. Int.* **2012**, *61*, 374.
- [5] H. Sirringhaus, *Adv. Mater.* **2005**, *17*, 2411.
- [6] J. Smith, R. Hamilton, Y. Qi, A. Kahn, D. D. C. Bradley, M. Heaney, I. McCulloch, T. D. Anthopoulos, *Adv. Funct. Mater.* **2010**, *20*, 2330.
- [7] Y. Diao, B. C.-K. Tee, G. Giri, J. Xu, D. H. Kim, H. A. Becerril, R. M. Stoltenberg, T. H. Lee, G. Xue, S. C. B. Mannsfeld, Z. Bao, *Nat. Mater.* **2013**, *12*, 665.
- [8] D. Yoo, Y. Kim, M. Min, G. H. Ahn, D. H. Lien, J. Jang, H. Jeong, Y. Song, S. Chung, A. Javey, T. Lee, *ACS Nano* **2018**, *12*, 11062.
- [9] M. Kaltenbrunner, T. Sekitani, J. Reeder, T. Yokota, K. Kuribara, T. Tokuhara, M. Drack, R. Schwödiauer, I. Graz, S. Bauer-Gogonea, S. Bauer, T. Someya, *Nature* **2013**, *499*, 458.
- [10] H. Jinno, K. Fukuda, X. Xu, S. Park, Y. Suzuki, M. Koizumi, T. Yokota, I. Osaka, K. Takimiya, T. Someya, *Nat. Energy* **2017**, *2*, 780.
- [11] A. Sandström, H. F. Dam, F. C. Krebs, L. Edman, *Nat. Commun.* **2012**, *3*, 1002.
- [12] A. Lafuma, D. Quéré, *Nat. Mater.* **2003**, *2*, 457.
- [13] Y. Lu, S. Sathasivam, J. Song, C. R. Crick, C. J. Carmalt, I. P. Parkin, *Science* **2015**, *347*, 1132.
- [14] A. Nakajima, A. Fujishima, K. Hashimoto, T. Watanabe, *Adv. Mater.* **1999**, *11*, 1365.
- [15] X. Deng, L. Mammen, H.-J. Butt, D. Vollmer, *Science* **2012**, *335*, 67.
- [16] Y. Rahmawan, L. Xu, S. Yang, *J. Mater. Chem. A* **2013**, *1*, 2955.
- [17] L. Xu, R. G. Karunakaran, J. Guo, S. Yang, *ACS Appl. Mater. Interfaces* **2012**, *4*, 1118.
- [18] R. G. Karunakaran, C.-H. Lu, Z. Zhang, S. Yang, *Langmuir* **2011**, *27*, 4594.
- [19] C.-Y. Wang, H. Groenzin, M. J. Shultz, *Langmuir* **2003**, *19*, 7330.
- [20] Y. Lai, Y. Tang, J. Gong, D. Gong, L. Chi, C. Lin, Z. Chen, *J. Mater. Chem.* **2012**, *22*, 7420.
- [21] L. Feng, S. Li, Y. Li, H. Li, L. Zhang, J. Zhai, Y. Song, B. Liu, L. Jiang, D. Zhu, *Adv. Mater.* **2002**, *14*, 1857.
- [22] T. Nishino, M. Meguro, K. Nakamae, M. Matsushita, Y. Ueda, *Langmuir* **1999**, *15*, 4321.
- [23] A. A. Zakhidov, J.-K. Lee, H. H. Fong, J. A. DeFranco, M. Chatzichristidi, P. G. Taylor, C. K. Ober, G. G. Malliaras, *Adv. Mater.* **2008**, *20*, 3481.
- [24] A. V. Rao, S. S. Latthe, D. Y. Nadargi, H. Hirashima, V. Ganesan, *J. Colloid Interface Sci.* **2009**, *332*, 484.
- [25] J. Fresnais, J. P. Chapel, F. Poncin-Epaillard, *Surf. Coat. Technol.* **2006**, *200*, 5296.
- [26] S. Gao, X. Dong, J. Huang, S. Li, Y. Li, Z. Chen, Y. Lai, *Chem. Eng. J.* **2018**, *333*, 621.
- [27] J. Bravo, L. Zhai, Z. Wu, R. E. Cohen, M. F. Rubner, *Langmuir* **2007**, *23*, 7293.
- [28] M. D. Lechner, *J. Serb. Chem. Soc.* **2005**, *70*, 361.
- [29] C. Luo, M. Xiang, X. Liu, H. Wang, *Microfluid. Nanofluid.* **2011**, *10*, 831.
- [30] T. Liu, C. J. Kim, *Science* **2014**, *346*, 1096.
- [31] A. W. Nørgaard, K. A. Jensen, C. Janfelt, F. R. Lauritsen, P. A. Clausen, P. Wolkoff, *Environ. Sci. Technol.* **2009**, *43*, 7824.